

Deep Learning-aided Parkinson’s Disease Diagnosis from Handwritten Dynamics

Clayton R. Pereira

Department of Computing
Federal University of São Carlos
São Carlos - SP, Brazil
claytontey@gmail.com

Silke A. T. Weber

Medical School of Botucatu
São Paulo State University
Botucatu - SP, Brazil
silke@fmb.unesp.br

Christian Hook

Fakultät Informatik/Mathematik
Ostbayerische Tech. Hochschule
Regensburg, Germany
christian.hook@hs-regensburg.de

Gustavo H. Rosa, João Papa

Department of Computing
São Paulo State University
Bauru - SP, Brazil
gth.rosa@uol.com.br
papa@fc.unesp.br

Abstract—Parkinson’s Disease (PD) automatic identification in early stages is one of the most challenging medicine-related tasks to date, since a patient may have a similar behaviour to that of a healthy individual at the very early stage of the disease. In this work, we cope with PD automatic identification by means of a Convolutional Neural Network (CNN), which aims at learning features from a signal extracted during the individual’s exam by means of a smart pen composed of a series of sensors that can extract information from handwritten dynamics. We have shown CNNs are able to learn relevant information, thus outperforming results obtained from raw data. Also, this work aimed at building a public dataset to be used by researchers worldwide in order to foster PD-related research.

Keywords-Parkinson’s Disease, Convolutional Neural Network

I. INTRODUCTION

Parkinson’s disease (PD) is a chronic, progressive, multi-lesion and neurodegenerative disease caused by the loss of a neurotransmitter called dopamine [1]. Usually, PD is more common in the elderly population, producing alterations in gait and posture that may increase the risk of falls and lead to mobility disabilities. As such, it impacts daily activities and reduces the quality of life concerning patients and their families [2], [3], [4].

Although some well-known drugs can help coping with the disease in early stages, their usage along the years might hasten neurodegeneration [5]. Therefore, a number of researchers from different domains aim at combining knowledge in order to aid PD diagnosis as early as possible. Due to their emerging use in a number of applications, decision-making techniques based on machine learning might be the most fruitful ones to deal with PD recognition [6].

Das et al. [7], for instance, presented a comparison among some classification techniques concerning PD diagnosis, achieving around 92.2% of classification accuracy by means of Neural Networks. Spadotto et al. [8] introduced the Optimum-Path Forest (OPF) [9], [10] in the context of automatic PD identification, and Gharehchopogh et al. [11] used Artificial Neural Networks with Multi-Layer Perceptron to diagnose the effects caused by Parkinson’s Disease. Spadotto et al. [12] also considered using a meta-heuristic-driven feature selection aiming at recognizing such illness.

Other works, such as the one by Pan et al. [13], analyzed the performance of Support Vector Machines with Radial Basis Function in order to compare the onset of tremor in patients with PD. Later on, Peker et al. [14] used sound-based features and complex-valued neural networks to aid PD diagnosis as well, and Hariharan et al. [15] developed a new feature weighting method using Model-based clustering (Gaussian mixture model) in order to enrich the discriminative ability of the dysphonia-based features, thus achieving 100% of classification accuracy.

However, most works make use of audio-based datasets to cope with PD identification. Very recently, Pereira et al. [16] proposed to aid PD diagnosis by means of handwriting movements. In addition, the very same group of authors made available a dataset with hundreds of images containing handwriting drawings made by both healthy individuals and patients. Since the writing ability is affected by Parkinson’s Disease, it is very usual to find such exams in hospitals and clinics, but only a few works have considered them for automatic diagnostic purposes.

Some years ago, a group of German researchers developed a very clever way to assist PD diagnosis: the so-called Biometric Smart Pen - *BiSP*[®] [17], which is essentially a pen composed of sensors that measure some information captured during handwritten exams. Although the pen has been originally designed for biometric purposes, it was further employed to aid PD diagnosis. Some years ago, Peuker et al. [18] used the signals extracted from the pen to perform PD identification, obtaining very suitable results. However, the authors extracted around 400 hand-crafted features from the signal, which were obtained by means of a sequential-driven feature selection algorithm, which may be too costly.

In this work, we proposed to learn pen-based features by means of a Convolutional Neural Network (CNN) [19], which can process information through a set of layers, being each one in charge of learning a different and finer representation. Moreover, as far as we are concerned, we have not noticed any work that deal with automatic PD diagnosis by means of deep learning techniques, which turns out to be the main contribution of this work. Additionally, another main contribution of this work is to make available a dataset composed of the signals extracted from patients and healthy individuals through

the smart pen.

The remainder of this paper is organized as follows. Sections II and III present some theoretical background with respect to CNNs and the methodology employed in this work, respectively. Section IV presents the experimental results, and Section V states conclusions and future works.

II. CONVOLUTIONAL NEURAL NETWORKS

Convolutional Neural Networks can be seen as a representation of a bigger class of models based on the Hubel's and Wiesel's architecture, which was presented in a seminal study in 1962 concerning the primary cortex of cats. This research has identified, basically, two kinds of cells: (i) *simple cells*, which possess an analogous duty to the filter bank step, and (ii) the *complex cells*, which perform a similar job to the CNN sampling step.

The first model that simulated a computer-based convolutional neural network was the well-known "Neocognitron" [20], which implemented an unsupervised training algorithm during the filter bank step, followed by a supervised training algorithm applied in the last layer. Later on, LeCun et al. [19], [21] simplified this architecture by proposing the use of the Backpropagation algorithm to train the network in a supervised way. Thus, several applications that used CNN emerged in the subsequent decades.

Basically, a CNN can be understood as an N -layered image processing sequence. Thereby, given an input image¹, a CNN essentially extracts a high level representation of its, called *multispectral image*, whose pixel attributes are concatenated in a feature vector for later application of pattern recognition techniques. Figure 1 introduces the naive architecture of a Convolutional Neural Network.

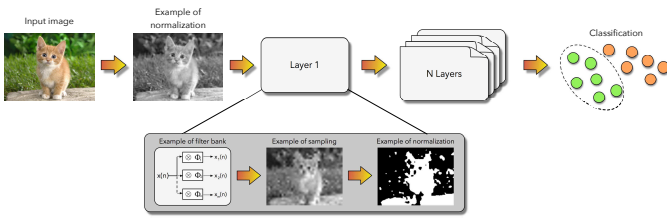


Fig. 1. A typical Convolutional Neural Network architecture.

As aforementioned, each CNN layer is often composed by three operations, being the first one a convolution with a filter bank, followed by a sampling phase and then by a normalization step. As one can observe in Figure 1, there is still a possibility of a normalization operation in the beginning of the whole process. The next sections describe in more details each of these steps.

A. Filter Bank

Let $\hat{I} = (D_I, \vec{I})$ be a multispectral image such that $D_I \in n \times n$ is the image domain, and $\vec{I} = \{I_1(p), I_2(p), \dots, I_m(p)\}$

¹The same procedure can be extended to signal processing-based applications.

corresponds to a pixel $p = (x_p, y_p) \in D_I$, and m stands for the number of bands. When \hat{I} is a grey-scale image, for instance, we have that $m = 1$ and $\hat{I} = (D_I, I)$.

Let $\phi = (\mathcal{A}, W)$ be a filter with weights $W(q)$ associated with every *pixel* $q \in \mathcal{A}(p)$, where $\mathcal{A}(p)$ denotes a mask of size $L_A \times L_A$, centered at p , and $q \in \mathcal{A}(p)$ if, and only if, $\max\{|x_q - x_p|, |y_q - y_p|\} \leq (L_A - 1)/2$. In case of multispectral filters, their weights can be depicted as vectors $\vec{W}_i(q) = \{w_{i,1}(q), w_{i,2}(q), \dots, w_{i,m}(q)\}$ for each filter i , and a multispectral filter bank can be then defined as $\phi = \{\phi_1, \phi_2, \dots, \phi_n\}$, where $\phi_i = (\mathcal{A}, \vec{W}_i)$, $i = \{1, 2, \dots, n\}$.

Thus, the convolution between an input image \hat{I} and a filter ϕ_i generates the band i of the filtered image $\hat{J} = (D_J, \vec{J})$, where $D_J \in D_I$ and $\vec{J} = \{J_1(p), J_2(p), \dots, J_n(p)\}$, $\forall p \in D_J$:

$$J_i(p) = \sum_{\forall q \in \mathcal{A}(p)} \vec{I}(q) \otimes \vec{W}_i(q), \quad (1)$$

where \otimes denotes the convolution operator. The weights of ϕ_i are usually generated from an uniform distribution, i.e., $U(0, 1)$, and afterwards normalized with mean zero and unitary norm.

B. Sampling

This operation has an extreme importance for a CNN, which intends to provide a translational invariance to the extracted features. Let $\mathcal{B}(p)$ be the sampling area of size $L_B \times L_B$ centered at p . Additionally, let $D_K = D_J/s$ be a regular sampling operation every s pixels. Therefore, the resulting sampling operation in the image $\hat{K} = (D_K, \vec{K})$ is defined as follows:

$$K_i(p) = \sqrt[n]{\sum_{\forall q \in \mathcal{B}(p)} J_i(q)^\alpha}, \quad (2)$$

where $p \in D_K$ denotes every pixel of the new image, $i = \{1, 2, \dots, n^2\}$, and α is a parameter that controls the operation sensitiveness.

C. Normalization

The last operation of a CNN is its normalization, which is a widely employed mechanism in order to enhance its performance [22]. This operation is based on the apparatus found on corticals neurons [23], being also defined under a squared-area $\mathcal{C}(p)$ of size $L_C \times L_C$ centered at pixel p , such as:

$$O_i(p) = \frac{K_i(p)}{\sum_{j=1}^n \sum_{\forall q \in \mathcal{C}(p)} K_j(q) K_i(q)}. \quad (3)$$

Thus, the above operation is accomplished for each pixel $p \in D_O \subset D_k$ of the resulting image $\hat{O} = (D_O, \vec{O})$.

III. METHODOLOGY

In this section, we present the methodology used to design the dataset, as well as the proposed approach to analyze the pen-based features (signals) by means of CNNs. In addition, we present the experimental setup as well.

A. HandPD Dataset

The writing of parkinsonian patients is often distorted and smaller (micro-graphing) than that of healthy individuals due to the tremors, reduced movement amplitudes, slowness and rigidity [24]. Currently, it is not straightforward to pinpoint a specific exam that can identify a patient in the early stages. Also, PD can be misidentified with other brain disorders.

Recently, Pereira et al. [16] built a dataset² concerning images acquired during handwriting exams, which aim at describing an individual skills when filling a form out, as the one depicted in Figure 2. The idea of the form is to ask a person to perform some specific tasks that are supposed nontrivial to PD patients, such as drawing “spirals” (row ‘c’ in Figure 2), “meanders” (row ‘d’ in Figure 2), and performing the so-called diadochokinese test, which is basically a test where the individual holds the pen with straight arms and perform hand-wrist movements. Since there are no drawings involved, only the signal generated through these movements are recorded by the pen.

Fig. 2. Form used to assess the handwritten skills of a given individual.

The former HandPD dataset was collected at the Faculty of Medicine of Botucatu, São Paulo State University, Brazil,

²<http://www.fc.unesp.br/~papa/pub/datasets/Handpd>

being composed of images extracted from handwriting exams of individuals divided into two groups: (i) healthy people and (ii) PD patients. In this work, we proposed to extend the original HandPD dataset with signals extracted from the smart pen as well. Figure 3 displays an image of the *BiSP*[®] used in this work. The signals generated by the pen concern six sensors, as described above:

- CH 1: Microphone;
- CH 2: Fingergrip;
- CH 3: Axial Pressure of ink Refill;
- CH 4: Tilt and Acceleration in “X direction”;
- CH 5: Tilt and Acceleration in “Y direction”;
- CH 6: Tilt and Acceleration “Z direction”.

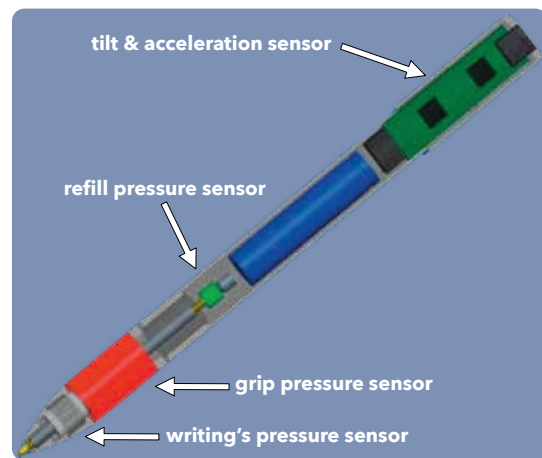


Fig. 3. Biometric Pen: sensors are located at four different points (extracted from [25]).

The difference between the exams of healthy individuals and patients are due to a dysfunction of movement disorders. The parkinsonian patients, for instance, present high levels of tremor during drawing tasks. Since each sensor outputs the whole signal acquired during the exam³, we can represent such data as a time series, as depicted in Figure 4, which represents the output of an exam from a healthy individual when drawing a spiral (e.g. Figure 7a). We can observe the drawing is pretty much the standard form of the image, while the signal extracted from the patient seems to be too much noisy, as displayed in Figure 5 (e.g. Figure 7b).

In order to build this initial dataset⁴, we used signals extracted from spirals and meanders only. The new dataset comprises 35 individuals, being 14 patients (10 males and 4 females) and 21 control (healthy) individuals (11 males and 10 females). Each person is asked to fill the form out using the smart pen starting from inward to outward. This activity concerns the analysis of the movement provided by spirals and meanders drawings, which quantify the normal motor activity

³The extension of the exam is defined as the time interval between a computer beep (a start call) and the end of the drawing process.

⁴We are now working on to expand the dataset with the diadochokinese and circles test (row “ab” in Figure 2).

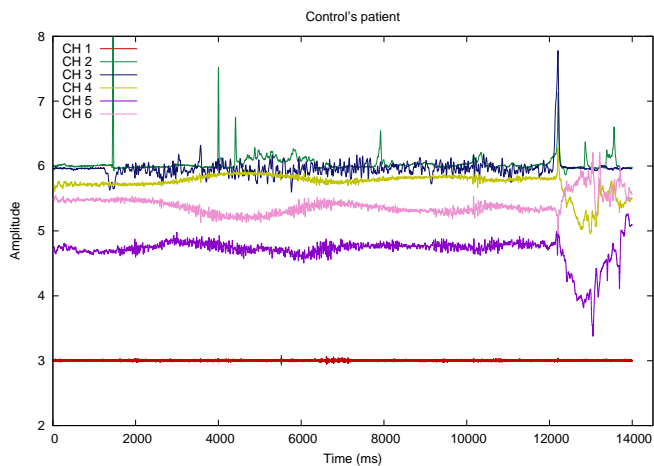


Fig. 4. Signals recorded by the pen from a control individual when drawing a spiral.

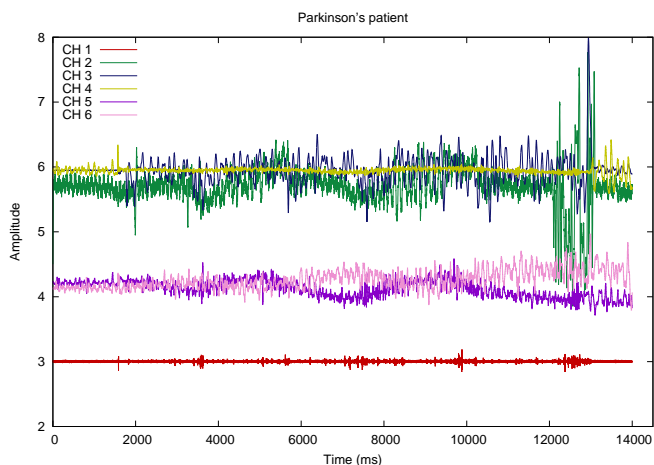


Fig. 5. Signals recorded by the pen from a PD patient when drawing a spiral.

in a healthy individual, as well as the dysfunction of PD patients.

B. Modelling Time Series in CNNs

We propose to model the problem of distinguishing PD and control individuals as an image recognition task by means of CNNs. Roughly speaking, the signals provided by the smart pen are transformed into pictures. Each exam is composed of r rows (exam time in milliseconds) and 6 columns, which stand for the aforementioned 6 signal channels (e.g. sensors). Therefore, each exam needs to be resized to a squared matrix in order to fulfil our purposes (notice the number of rows r may differ from each test, since a person may take longer than another to perform the exam). After rescaling, each exam-based matrix is then normalized in order to be modelled as a gray-scale image. Figures 6 and 7 illustrate some drawings and their transformed versions into time series-based images. One can observe the different patterns between spiral and meander images, as well as different patterns between the same drawings of healthy and PD patients.

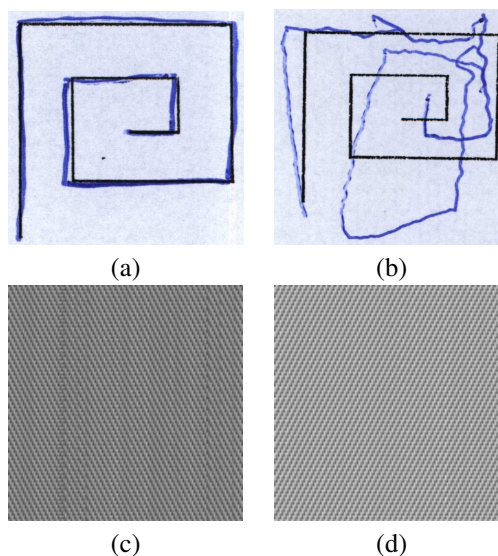


Fig. 6. Meander samples from: (a) control and (b) PD patient, and their respective time series-based images in (c) and (d).

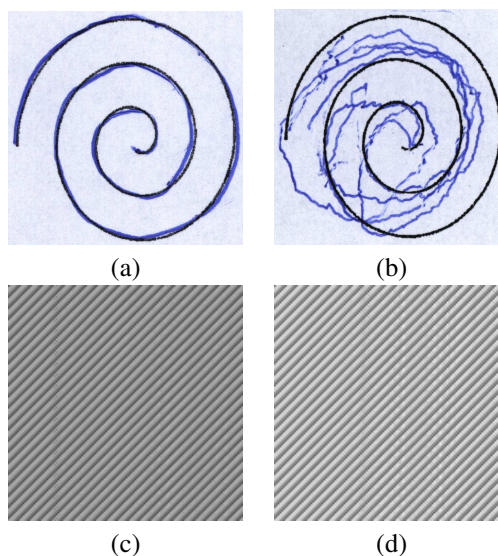


Fig. 7. Spiral samples from: (a) control and (b) PD patient, and their respective time series-based images in (c) and (d).

C. Experimental Setup

In this work, we classified meanders and spirals images drawn by the control group and PD patients using a CNN-based approach. Also, we conducted an additional experiment over the raw data to serve as a baseline for comparison purposes. Although one can use any supervised machine learning technique, we opted to employ the OPF classifier, which is a fast and parameterless technique [9], [10].

We divided the experiments into two datasets: (i) the meanders and the (ii) spirals. Both datasets are composed of 308 images, being 224 PD patients and 84 control group samples. In addition, we evaluated the robustness of CNNs over two different image resolutions: 64×64 and 128×128 pixels. Also, we evaluate the influence of the training set size over two

distinct experiments: one with 75% of the dataset for training and 25% for testing, and another with 50% for training and 50% for testing purposes.

In regard to the source-code, we used the well-known Caffe library⁵ [26], which is developed under GPGPU (General-Purpose computing on Graphics Processor Units) platform, thus providing more efficient implementations. Each experiment was evaluated by a different CNN architecture provided by Caffe using 10,000 training iterations with mini-batches of size 16. In order to provide a statistical analysis by means of Wilcoxon signed-rank test with significance of 0.05 [27], we conducted a cross-validation with 20 runnings. Different CNN architectures were used to provide a deeper experimental analysis:

- 1) ImageNet: composed of 5 convolution layers, 5 pooling layers and 2 normalization layers. It is also constituted by 5 ReLU layers among the convolution ones, 2 inner product layers, 2 dropout layers, 1 softmax loss layer and 1 accuracy layer for testing purposes.
- 2) CIFAR-10: a quick version is used, composed of 3 convolution layers and 3 pooling layers. It is also constituted by 3 ReLU layers among the convolution ones, 2 inner product layers, 1 softmax loss layer and 1 accuracy layer for testing intentions.
- 3) LeNet: composed of 2 convolution layers and 2 pooling layers. It is also constituted by 2 inner product layers and a single ReLU layer among the inner product ones. Finally, we have 1 softmax loss layer and 1 accuracy layer for testing duties.

Since the images used in the experiments are domain-specific, we did not employ transfer learning, i.e. we opted to train the networks using our own datasets.

IV. EXPERIMENTAL RESULTS

This section aims at presenting the experimental results concerning the CNN-based Parkinson’s Disease identification. As aforementioned in Section III-C, we compared three distinct CNN architectures and a baseline approach by means of the OPF classifier considering both meander and spiral datasets. Tables I and II describe the average results regarding meander dataset. The most accurate results, according to Wilcoxon signed-rank test, are in bold. Table I presents the overall accuracy, while Table II presents the recognition rates per class. Notice the overall accuracy is computed using the standard formulation, i.e., $(1 - \frac{errors}{dataset\ size}) * 100$.

	50% / 50% (Train / Test)		75% / 25% (Train / Test)	
	64 × 64	128 × 128	64 × 64	128 × 128
ImageNet	86.14%	84.74%	85.00%	87.14%
CIFAR-10	56.59%	50.00%	68.83%	64.22%
LeNet	25.45%	40.00%	43.64%	36.36%
OPF	79.87%	76.62%	84.42%	81.82%

TABLE I
AVERAGE OVERALL ACCURACY OVER THE TEST SET CONSIDERING MEANDER DATASET.

One can observe CNN-based features obtained the most accurate results for all experiments, except for the 75% – 25% experiment with 64 × 64 images. Probably, images with such resolution may not represent the whole time series well enough to be discriminated by CNNs. Also, the best results were obtained by ImageNet architecture with 128 × 128 images and using 75% of the dataset for training purposes. Since LeNet is shallower than ImageNet and CIFAR-10 architectures, it obtained the lowest accuracy recognition rates.

Table II presents the results per class. Since our dataset is not balanced, it is quite useful to provide the recognition rates considering both healthy and patients group. In general, the recognition rates are quite good, being the bottleneck of the proposed approach the recognition rates over control individuals. Although we have more control people than PD patients, a considerable number of healthy individuals were classified as patients, since the dataset comprises PD patients with exams quite close to the ones performed by healthy individuals. As aforementioned, one of the greatest challenges in PD identification concerns the early stage of the disease, where both patients and healthy individuals have similar handwritten skills.

	50% / 50% (Train / Test)				75% / 25% (Train / Test)			
	64 × 64		128 × 128		64 × 64		128 × 128	
	Control	PD	Control	PD	Control	PD	Control	PD
ImageNet	74.29%	90.58%	76.31%	87.90%	72.86%	89.55%	76.19%	91.25%
CIFAR-10	15.71%	71.92%	10.00%	65.00%	33.33%	82.14%	10.95%	84.20%
LeNet	00.00%	35.00%	00.00%	55.00%	00.00%	60.00%	00.00%	50.00%
OPF	61.91%	86.61%	52.38%	85.71%	61.91%	92.86%	52.38%	92.86%

TABLE II
AVERAGE CONTROL AND PD PATIENTS ACCURACIES OVER THE TEST SET CONSIDERING MEANDER DATASET.

Tables III and IV present the results concerning spirals dataset. In this case, OPF over the raw data obtained better results than the ones achieved over meanders. The most accurate result of 83.77% was obtained by OPF with 64 × 64 images using 50% of the dataset for training purposes. The best results concerning CNNs were obtained using 75% for the training set, which is somehow expected, since the main shortcoming of deep learning techniques is related to the dataset size for training. Once again, the shallower architecture (LeNet) obtained the lowest recognition rates.

	50% / 50% (Train / Test)		75% / 25% (Train / Test)	
	64 × 64	128 × 128	64 × 64	128 × 128
ImageNet	78.41%	77.69%	80.19%	77.53%
CIFAR-10	75.58%	73.38%	78.31%	70.78%
LeNet	54.55%	40.00%	43.64%	40.00%
OPF	83.77%	80.52%	79.22%	77.92%

TABLE III
AVERAGE OVERALL ACCURACY OVER THE TEST SET CONSIDERING SPIRAL DATASET.

Table IV presents the accuracy results per class. Once again, the recognition rates for each group are considerably good, with CNNs obtaining around 98% of classification rate concerning PD patients, and OPF achieving around 71% of recognition rate for the control group. In this case, smaller

⁵<http://caffe.berkeleyvision.org>

training sets seemed to be fruitful for CNNs, since spirals pose a greater challenge than meanders. In this case, it is possible to distinguish PD patients from healthy individual with less images. Notice the results over spirals are considerably more accurate than the ones obtained over meanders, as well as a shallower architecture (CIFAR-10) obtained the best results in some situations.

	50% / 50% (Train / Test)				75% / 25% (Train / Test)			
	64 × 64		128 × 128		64 × 64		128 × 128	
	Control	PD	Control	PD	Control	PD	Control	PD
ImageNet	58.10%	86.03%	56.19%	85.76%	59.52%	87.95%	55.48%	85.80%
CIFAR-10	29.76%	92.77%	06.31%	98.53%	57.38%	86.16%	14.76%	91.79%
LeNet	00.00%	75.00%	00.00%	55.00%	00.00%	60.00%	00.00%	55.00%
OPF	66.67%	90.18%	61.91%	87.50%	71.43%	87.50%	66.67%	82.14%

TABLE IV
AVERAGE CONTROL AND PD PATIENTS ACCURACIES OVER THE TEST SET CONSIDERING SPIRAL DATASET.

Also, one interest result that can be observed refers to how OPF performed better on a smaller training set. As we are working with signals converted into images, some of the PD patients are still not impaired, resulting in similar signals to a control group patient. Furthermore, there are more training samples from parkinson's group than that of control group ones. Thus, the raw data considering PD patients and healthy individuals may look similar at certain points.

V. CONCLUSIONS

In this paper, we cope with the problem of PD identification by means of Convolutional Neural Networks. Basically, the idea is to model the handwritten dynamics as a time series, and to use it as an input to a CNN, which will be able to learn features that are used to distinguish healthy individuals from PD patients. The main contributions of this paper rely on two main aspects: (i) to employ a deep learning-oriented approach to aid Parkinson's Disease diagnosis, (ii) as well as to design a signal-based dataset composed of features related to handwritten dynamics.

The experimental section comprised different CNN architectures, as well as images with different resolutions and distinct training set sizes. The results obtained by CNNs were compared against the raw data classified by means of the OPF, and showed to be very promising, since CNNs were able to learn important features to differentiate PD patients from healthy individuals, thus obtaining very good results over the datasets.

In regard to future works, we aim at extending the dataset with more exams (circles and diadochokinese test), as well as to increase the number of individuals. Also, our next idea is to learn a fusion schema that considers all exams when making decisions about an individual. Also, we aim at employing different approaches to transform temporal series into 2D images, such as the visual rhythms proposed by Almeida et al. [28].

ACKNOWLEDGMENT

The authors would like to thank FAPESP grants #2010/15566-1, #2014/16250-9 and #2015/25739-4, Capes,

and CNPq grant #306166/2014-3.

REFERENCES

- [1] A. J. Lees, J. Hardy, and T. Revesz, "Parkinson's disease," *The Lancet*, vol. 373, no. 9680, pp. 2055–2066, 2009.
- [2] B. E. Maki and W. E. McIlroy, "Change-in-support balance reactions in older persons: An emerging research area of clinical importance," *Neurologic Clinics*, vol. 23, no. 3, pp. 751–783, 2005.
- [3] G. F. Marchetti and S. L. Whitney, "Older adults and balance dysfunction," *Neurologic Clinics*, vol. 23, no. 3, pp. 785–805, aug 2005.
- [4] Y. J. Zhao, L. C. S. Tan, P. N. Lau, W. L. Au, S. C. Li, and N. Luo, "Factors affecting health-related quality of life amongst asian patients with parkinson's disease," *European Journal of Neurology*, vol. 15, no. 7, pp. 737–742, jul 2008.
- [5] S. Fahn, D. Oakes, I. Shoulson, K. Kieburtz, A. Rudolph, A. Lang, C. W. Olanow, C. Tanner, K. Marek, and Parkinson Study Group, "Levodopa and the progression of parkinson's disease," *The New England journal of medicine*, vol. 351, no. 24, pp. 2498–2508, 2004.
- [6] B. E. Sakar, M. E. Isenkul, C. O. Sakar, A. Sertbas, F. Gurgun, S. Delil, H. Apaydin, and O. Kursun, "Collection and analysis of a parkinson speech dataset with multiple types of sound recordings," *IEEE Journal of Biomedical and Health Informatics*, vol. 17, pp. 828–834, 2013.
- [7] R. Das, "A comparison of multiple classification methods for diagnosis of parkinson disease," *Expert Systems with Applications*, vol. 37, no. 2, pp. 1568 – 1572, 2010.
- [8] A. A. Spadotto, R. C. Guido, J. P. Papa, and A. X. Falcão, "Parkinson's disease identification through optimum-path forest," in *International Conference of the IEEE Engineering in Medicine and Biology Society*, 2010, pp. 6087–6090.
- [9] J. P. Papa, A. X. Falcão, and C. T. N. Suzuki, "Supervised pattern classification based on optimum-path forest," *International Journal of Imaging Systems and Technology*, vol. 19, no. 2, pp. 120–131, 2009.
- [10] J. P. Papa, A. X. Falcão, V. H. C. Albuquerque, and J. M. R. S. Tavares, "Efficient supervised optimum-path forest classification for large datasets," *Pattern Recognition*, vol. 45, no. 1, pp. 512–520, 2012.
- [11] F. S. Gharehchopogh and P. Mohammadi, "Article: A case study of parkinsons disease diagnosis using artificial neural networks," *International Journal of Computer Applications*, vol. 73, no. 19, pp. 1–6, 2013.
- [12] A. A. Spadotto, R. C. Guido, R. F. Carnevali, A. F. Pagnin, J. P. Papa, and A. X. Falcão, "Improving parkinson's disease identification through evolutionary-based feature selection," in *International Conference of the IEEE Engineering in Medicine and Biology Society*, 2010, pp. 7857–7860.
- [13] S. Pan, S. Iplikci, K. Warwick, and T. Z. Aziz, "Parkinson's disease tremor classification, a comparison between support vector machines and neural networks," *Expert Systems with Applications*, vol. 19, pp. 10764–10771, 2012.
- [14] M. Peker, B. Sen, and D. Delen, "Computer-aided diagnosis of parkinson's disease using complex-valued neural networks and mRMR feature selection algorithm," *Journal of Healthcare Engineering*, vol. 6, no. 3, pp. 281–302, 2015.
- [15] M. Hariharan, K. Polat, and R. Sindhu, "A new hybrid intelligent system for accurate detection of parkinson's disease," *Computer Methods and Programs in Biomedicin*, vol. 11, no. 3, pp. 904–913, 2014.
- [16] C. R. Pereira, D. R. Pereira, F. A. da Silva, C. Hook, S. A. T. Weber, L. A. M. Pereira, and J. P. Papa, "A step towards the automated diagnosis of parkinson's disease: Analyzing handwriting movements," in *IEEE 28th International Symposium on Computer-Based Medical Systems*, 2015, pp. 171–176.
- [17] G. University of Applied Sciences Team, Regensburg. (2002) A novel multisensoric system recording and analyzing human biometric features for biometric and biomedical applications. [Online]. Available: <http://www.bisp-regensburg.de/references.html>
- [18] D. Peuker, G. Scharfenberg, and C. Hook, "Feature selection for the detection of fine motor movement disorders in parkinson's patients," in *Advanced Research Conference*, ser. ARC '11. Shaker Verlag, 2011.
- [19] Y. LeCun, B. Boser, J. S. Denker, D. Henderson, R. E. Howard, W. Hubbard, and L. D. Jackel, "Backpropagation applied to handwritten zip code recognition," *Neural Computation*, vol. 1, no. 4, pp. 541–551, 1989.
- [20] K. Fukushima and S. Miyake, "Neocognitron: A new algorithm for pattern recognition tolerant of deformations and shifts in position," *Pattern Recognition*, vol. 15, no. 6, pp. 455–469, 1982.

- [21] Y. LeCun, B. Boser, J. S. Denker, R. E. Howard, W. Hubbard, L. D. Jackel, and D. Henderson, "Advances in neural information processing systems 2," D. S. Touretzky, Ed. San Francisco, CA, USA: Morgan Kaufmann Publishers Inc., 1990, ch. Handwritten Digit Recognition with a Back-propagation Network, pp. 396–404.
- [22] D. Cox and N. Pinto, "Beyond simple features: A large-scale feature search approach to unconstrained face recognition," in *Proceedings of the IEEE International Conference on Automatic Face Gesture Recognition and Workshops*, 2011, pp. 8–15.
- [23] W. Geisler and D. Albrecht, "Cortical neurons: isolation of contrast gain control," *Vision Research*, vol. 32, no. 8, pp. 1409–1410, 1992.
- [24] W. A. V. Gemmert, H. L. Teulings, and G. E. Stelmach, "Parkinsonian patients reduce their stroke size with increased processing demands," *Brain and Cognition*, vol. 47, no. 3, pp. 504–512, dec 2001.
- [25] D. Peueker, G. Scharfenberg, and C. Hook, "Feature selection for the detection of fine motor movement disorders in parkinsons patients," in *Advanced Research Conference 2011*, 2011.
- [26] Y. Jia, E. Shelhamer, J. Donahue, S. Karayev, J. Long, R. Girshick, S. Guadarrama, and T. D. T., "Caffe: Convolutional architecture for fast feature embedding," *arXiv preprint arXiv:1408.5093*, 2014.
- [27] F. Wilcoxon, "Individual comparisons by ranking methods," *Biometrics Bulletin*, vol. 1, no. 6, pp. 80–83, 1945.
- [28] J. G. Almeida, J. A. dos Santos, B. Alberton, L. P. C. Morellato, and R. S. Torres, "Phenological visual rhythms: Compact representations for fine-grained plant species identification," *Pattern Recognition Letters*, 2015.